Comparative Morphology of Changeable Skin Papillae in Octopus and Cuttlefish

Justine J. Allen,[1,2]* George R. R. Bell,[2] Alan M. Kuzirian,[2] Sachin S. Velankar,[3] and Roger T. Hanlon[2,4]

[1]*Department of Neuroscience, Brown University, Providence, Rhode Island 02912*
[2]*Program in Sensory Physiology and Behavior, Marine Biological Laboratory, Woods Hole, Massachusetts 02543*
[3]*Department of Chemical and Petroleum Engineering, University of Pittsburgh, Pittsburgh, Pennsylvania 15261*
[4]*Department of Ecology and Evolutionary Biology, Brown University, Providence, Rhode Island 02912*

ABSTRACT A major component of cephalopod adaptive camouflage behavior has rarely been studied: their ability to change the three-dimensionality of their skin by morphing their malleable dermal papillae. Recent work has established that simple, conical papillae in cuttlefish (*Sepia officinalis*) function as muscular hydrostats; that is, the muscles that extend a papilla also provide its structural support. We used brightfield and scanning electron microscopy to investigate and compare the functional morphology of nine types of papillae of different shapes, sizes and complexity in six species: *S. officinalis* small dorsal papillae, *Octopus vulgaris* small dorsal and ventral eye papillae, *Macrotritopus defilippi* dorsal eye papillae, *Abdopus aculeatus* major mantle papillae, *O. bimaculoides* arm, minor mantle, and dorsal eye papillae, and *S. apama* face ridge papillae. Most papillae have two sets of muscles responsible for extension: circular dermal erector muscles arranged in a concentric pattern to lift the papilla away from the body surface and horizontal dermal erector muscles to pull the papilla's perimeter toward its core and determine shape. A third set of muscles, retractors, appears to be responsible for pulling a papilla's apex down toward the body surface while stretching out its base. Connective tissue infiltrated with mucopolysaccharides assists with structural support. *S. apama* face ridge papillae are different: the contraction of erector muscles perpendicular to the ridge causes overlying tissues to buckle. In this case, mucopolysaccharide-rich connective tissue provides structural support. These six species possess changeable papillae that are diverse in size and shape, yet with one exception they share somewhat similar functional morphologies. Future research on papilla morphology, biomechanics and neural control in the many unexamined species of octopus and cuttlefish may uncover new principles of actuation in soft, flexible tissue. J. Morphol. 275:371–390, 2014. © 2013 Wiley Periodicals, Inc.

KEY WORDS: cephalopod; muscular hydrostat; muscle; texture; camouflage

INTRODUCTION

Coleoid cephalopods are preyed upon by a variety of visual predators: diving marine mammals and birds, teleost and cartilaginous fish, even other cephalopods (Clarke, 1996; Croxall and Prince, 1996; Hanlon and Messenger, 1996; Kla-ges, 1996; Smale, 1996; Hanlon, 2007). In response to predation pressure, octopus, squid and cuttlefish have evolved remarkable adaptive camouflage behaviors and can quickly change their appearance according to cues in their visual surroundings. These camouflage behaviors are multifaceted and include adjustments in color (Mäthger et al., 2008; Akkaynak et al., 2012), pattern (Hanlon and Messenger, 1988; Barbosa et al., 2004, 2008; Chiao et al., 2007, 2009, 2010; Kelman et al., 2007; Hanlon et al., 2009, 2011; Zylinski et al., 2009b), transparency (Zylinski and Johnsen, 2011), posture (Moynihan and Rodaniche, 1982; Bush et al., 2009; Barbosa et al., 2012), locomotion (Hanlon and Messenger, 1996; Huffard et al., 2005; Huffard, 2006; Zylinski et al., 2009a; Hanlon et al., 2010), and skin texture (Packard and Hochberg, 1977; Huffard, 2006; Allen et al., 2009, 2013). To date, most of this work has been done with the model species *Sepia officinalis*, Linnaeus the common European cuttlefish, but cephalopods are found throughout marine habitats and have diverged in response to a variety of ecological pressures (Boyle and Boletzky, 1996; Hanlon and Messenger, 1996). As a result, comparative studies can

provide insight into the way common selective pressures (in this case, visual predation) can provide convergent solutions.

Benthic coleoids (octopus and cuttlefish) have developed papillae to rapidly adjust their skin's three-dimensional texture according to their surroundings. This morphing ability allows the animal to resemble the physical texture of some natural substrates by creating false edges that disguise the animal's true outline with an "irregular marginal form," that is, structural or morphological complexity that conceals an animal's true shape (Cott, 1940; Stevens and Merilaita, 2009). In *S. officinalis*, papilla expression is driven by visual, not tactile cues (Hanlon and Messenger, 1988; Allen et al., 2009) and the functional morphology of one of the nine types of papillae found in that species was described recently (Allen et al., 2013). Like squid and octopus arms and tentacles (Kier, 1982, 1992, 2012; Kier and Smith, 1985; Smith and Kier, 1989; Kier and Thompson, 2003; Kier and Stella, 2007), small dorsal papillae were found to have design features of a muscular hydrostat where papilla extension and support were both provided by muscle fibers in the papilla's core. However, a mechanism for papilla retraction was not confirmed.

Papilla location and morphology are fixed within species, but papilla shape, size, and density vary greatly among benthic octopuses and cuttlefish (e.g., Packard and Sanders, 1971; Packard and Hochberg, 1977; Roper and Hochberg, 1988; Hanlon and Messenger, 1996; Norman, 2000; Allcock, 2005; Huffard, 2006; Allen et al., 2009). Presumably, the functional morphology of different papilla sizes and forms correlates with the behavioral ecology of the species, but this topic has yet to be studied in detail, especially in the field under natural conditions (Packard and Hochberg, 1977; Hanlon and Messenger, 1988; Roper and Hochberg, 1988). We used brightfield and scanning electron microscopy (SEM) to examine and compare the functional morphology among several papilla types from two cuttlefish and four octopus species: i) *Sepia officinalis* small dorsal papillae, ii) *Octopus vulgaris* small dorsal and ventral eye papillae, iii) *Macrotritopus defilippi* dorsal eye papillae, iv) *Abdopus aculeatus* major mantle papillae, v) *O. bimaculoides* arm, minor mantle, and dorsal eye papillae, and vi) *S. apama* face ridge papillae.

METHODS
Animals, Tissue Preparation, and Field Photographs

Sepia officinalis were hatched from eggs collected in the English Channel and maintained in the Marine Resources Center of the Marine Biological Laboratory, Woods Hole, Massachusetts, USA. Tissue from *Abdopus aculeatus* was collected from one animal used for an unrelated experiment. *S. apama* were maintained at the Sydney Institute of Marine Science, Mosman, New South Wales, Australia. Several animals were collected from the wild: three *Octopus vulgaris* and one *Macrotritopus defilippi* from Florida, and two *O. bimaculoides* from California. Animals were anesthetized with 3–5% ethanol in cold natural seawater (NSW) before sacrifice. Skin was dissected away from underlying musculature (~4 cm^2 pieces), then stretched and pinned to a Sylgard-lined Petri dish containing cold, 20 mmol l^{-1} Tris-buffered NSW (pH 8.0). Seawater was rapidly replaced with fixative: Hollande's variation of Bouin's, Karnovsky's, 2.5 or 4% paraformaldehyde. After a minimum of 18 h, the fixative was replaced with 20 mmol l^{-1} Tris-buffered NSW (pH 8.0) for storage.

Naturally behaving animals of each species were photographed under ambient lighting conditions at various field sites, except *A. aculeatus*, which were photographed in the laboratory.

Serial Sections

Individual papillae (or a small piece of papilla, in the case of *S. apama* face ridge papillae) were dissected from surrounding fixed tissue, dehydrated with an ethanol series, infiltrated, and embedded in polyester wax (Hallstar PEG 400 Distearate, melting point 36°C). The following number of samples were examined: *S. officinalis* small dorsal papillae, 12; *O. vulgaris* small dorsal papillae, 12; ventral eye papillae, two; *M. defilippi* dorsal eye papillae, two; *A. aculeatus* major mantle papillae, three; *O. bimaculoides* arm papillae, three; minor mantle papillae, six; and dorsal eye papillae, two; *S. apama* face ridge papillae, seven. A rotary microtome (Leica) was used to cut serial sections (6–10 μm thickness), in cross section or *en face* (from the apical tip toward the base), which were expanded and mounted using 2% paraformaldehyde on glass slides precoated with subbing solution (Weaver, 1955). Slides were allowed to dry before staining or sputtercoating for brightfield or SEM, respectively. [Norenburg and Barrett (1987) and Kier (1992) discussed similar methods in detail.]

Brightfield Microscopy: Stains

The following stains were used on serial sections to study the functional morphology of cuttlefish and octopus papillae: Mallory's triple connective tissue stain (Mallory's 1: acid fuchsin; Mallory's 2: aniline blue, orange G); Weigert's iron hematoxylin, Verhoff's elastin stain (potassium iodide, iodine, ferric chloride), Van Gieson's stain (saturated aqueous picric acid solution, acid fuchsin), and Müller's colloidal iron (colloidal iron, acetic acid, potassium ferrocyanide, hydrochloric acid). See Humason (1967) for procedures and figure legends for specific stain combinations. Stained sections were viewed with a Zeiss AxioSkop or Axiovert 135 and photographed with a Canon 5D-Mark II camera.

For all species, stain affinities were as follows. Mallory's triple connective tissue stain: light purple, blood vessel; brown or yellow, chromatophore pigment cell; blue, connective tissue (mostly collagen); light pink, epidermis; medium pink, muscle; very light purple, nerve; dark pink, reflective elements (leucophores and iridophores). Weigert's iron hematoxylin and Mallory's 2: brown or yellow, chromatophore pigment cell; blue, connective tissue (mostly collagen), light brown, epidermis (on perimeter); light brown, muscle; very light brown, nerve; orange, reflective elements (leucophores and iridophores). Verhoff's elastin stain: dark purple, epidermis (on perimeter); medium to dark purple, muscle; very dark purple, reflective elements (leucophores and iridophores). Müller's colloidal iron and Van Gieson's stain: medium pink, blood vessel; brown or yellow, chromatophore pigment cell; bright pink, collagen; medium pink, epidermis (on perimeter of sections); bright blue, mucopolysaccharide-rich (carboxymucins) connective tissue; bright blue, mucous vesicles in goblet cells (in epidermis); salmon, muscle; light pink, nerve; orange, reflective elements (leucophores and iridophores).
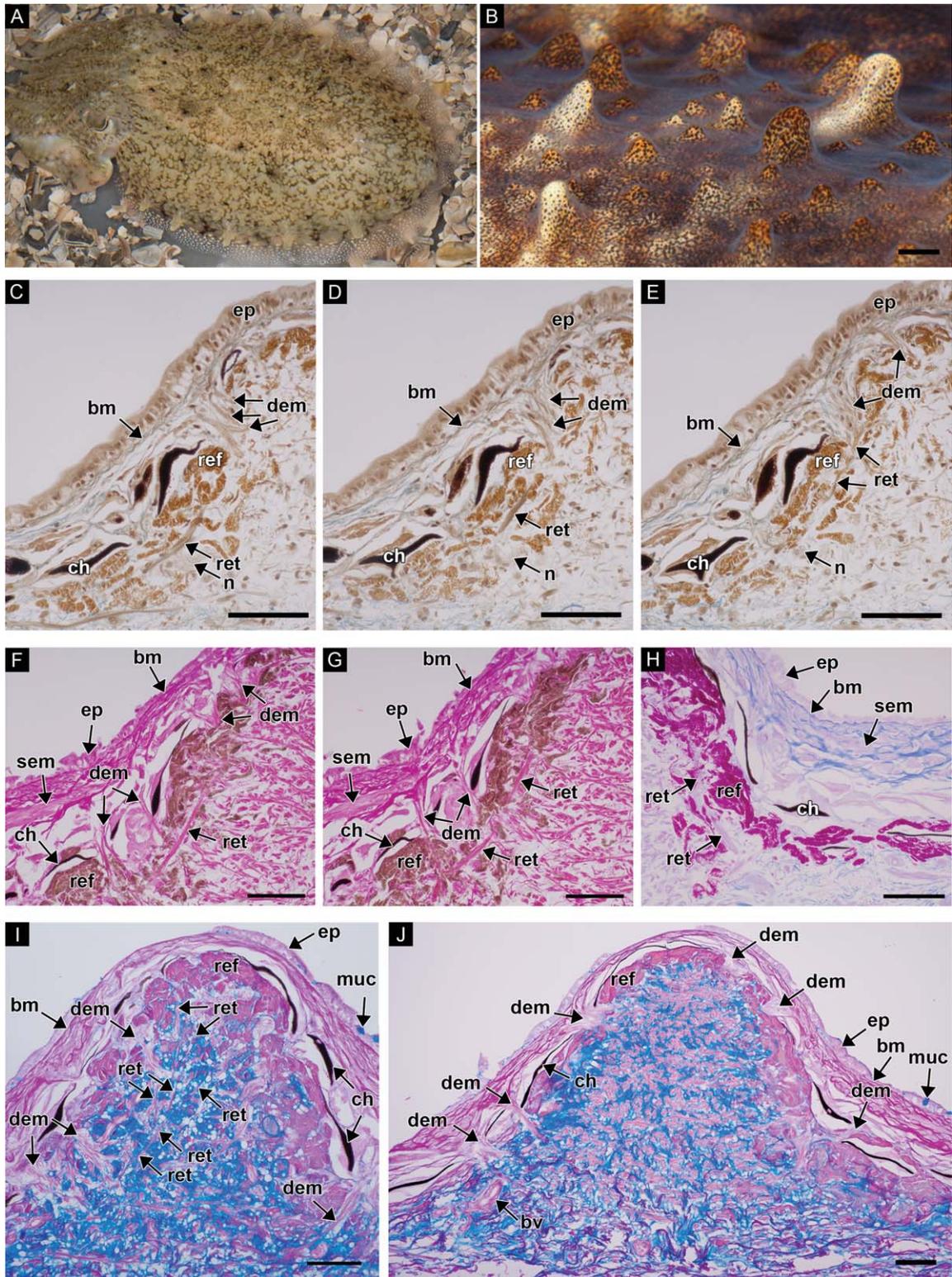
Fig. 1. (**A**) *Sepia officinalis* with many small dorsal papillae extended on the mantle, head and arms. (**B**) Close up of small dorsal papillae. (**C–J**) Cross sections of extended small dorsal papillae. (C–I) Retractor muscles were found between the reflective elements layer and the muscular core. (C–E) Adjacent serial sections stained with Weigert's iron hematoxylin and Mallory's 2. (F,G) Adjacent serial sections stained with Van Gieson's stain and impotent (expired) Verhoff's elastin stain. (H) Section stained with Mallory's triple connective tissue stain. (I,J) Staining with Müller's colloidal iron and Van Gieson's stain revealed mucopolysaccharide-rich connective tissue surrounding the erectors that make up the papilla's muscular core. (I) Section showing a retractor dividing to radiate near the apex of the papilla. Tissue types were identified by stain affinities and morphology: bm, basement membrane; ch, chromatophore; dem, dermal erector muscle; ep, epidermis; muc, mucus; n, nerve; ref, reflective element; ret, retractor muscle; sem, subepidermal muscles. Scale bars: (B) ~2 mm; (C–J) 100 μm.
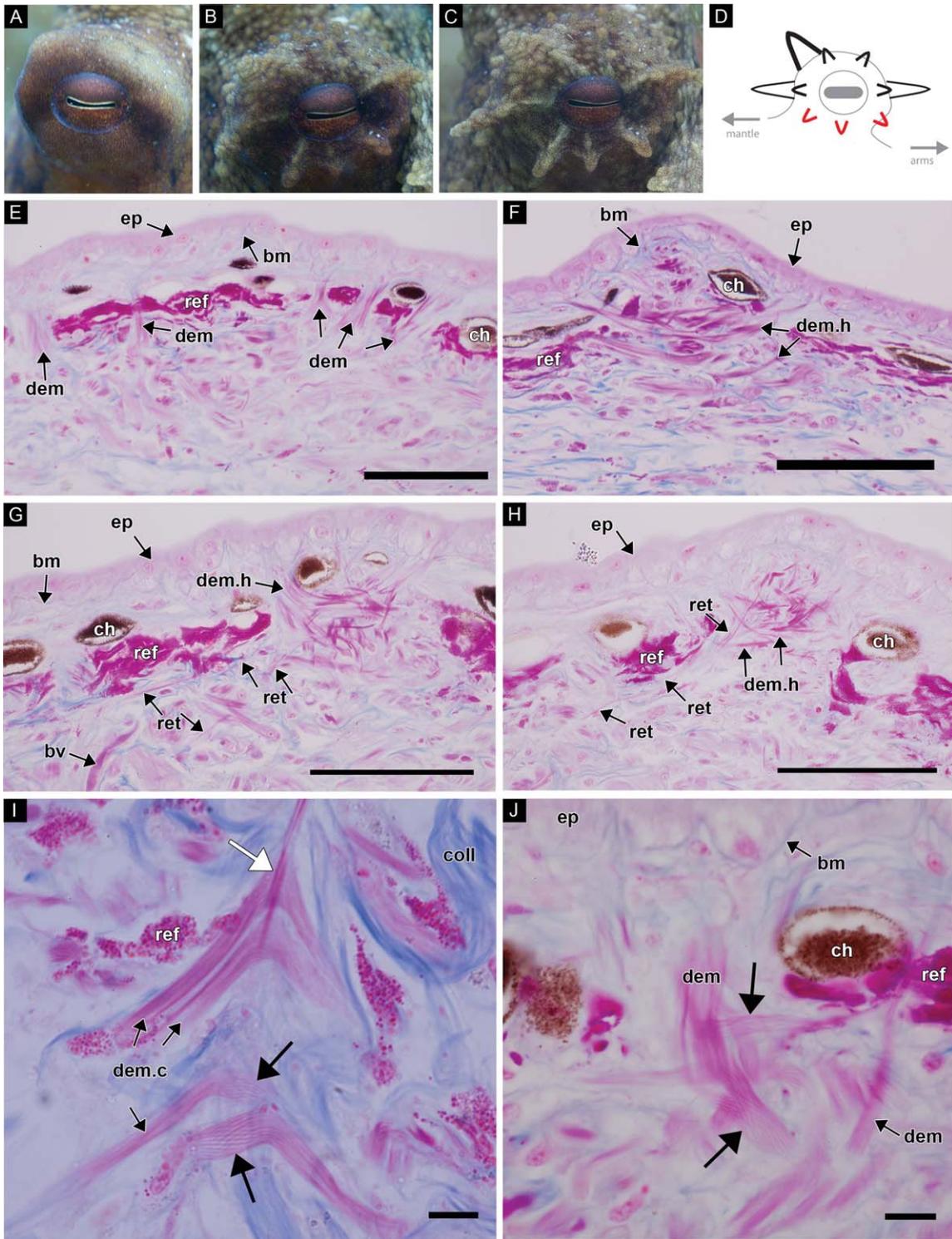
Fig. 2. *Octopus vulgaris* small dorsal papillae. (**A–C**) Field images of a live animal altering its appearance by changing the expression of the papillae around its eye. (**D**) Drawing of the primary papillae expressed in A-C showing the location of the ventral eye papillae (red); small dorsal papillae are interspersed among primary papillae (not shown, see B-C). (**E–J**) Small dorsal papillae stained with Mallory's triple connective tissue stain. (E,F) Cross sections of retracted (E) and extended (F) small dorsal papillae showing papilla elements, particularly horizontal erectors. (G,H) Serial cross sections showing papilla elements, particularly retractor muscles between the reflective elements and the muscular core. (I) *En face* section showing retractor muscles attached to circular dermal erector muscles (white arrow). Circular erectors were obliquely striated (large black arrows). (J) Cross section of an obliquely striated (large black arrows) small dorsal papilla erector connecting to the basement membrane of the epidermis. Tissue types were identified by stain affinities and morphology: bm, basement membrane; bv, blood vessel; ch, chromatophore; dem.c, circular dermal erector muscle; coll, collagen; dem, dermal erector muscle; dem.h, horizontal dermal erector muscle; ep, epidermis; ref, reflective elements; ret, retractor muscle. Scale bars: 100 μm.
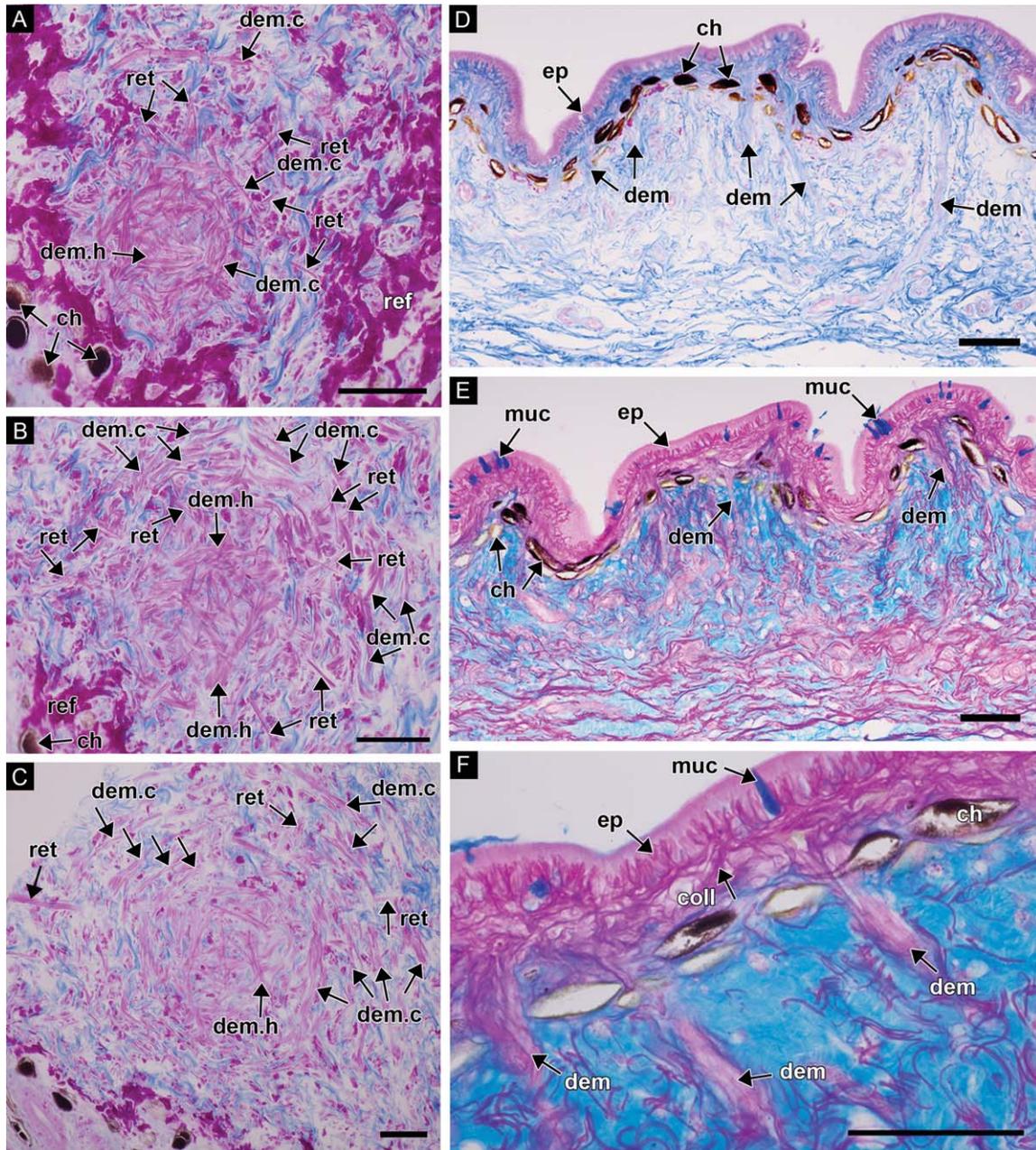
Fig. 3. *Octopus vulgaris* small dorsal and ventral eye papillae. (**A–C**) Selected sections from a small dorsal papilla cut *en face* showing papilla elements, particularly circular erectors and retractors. (**D–F**) Ventral eye papillae stained with Mallory's triple connective tissue stain (D) or Müller's colloidal iron and Van Gieson's stains (E–F). Apparent space (D) is actually filled with mucopolysaccharide-rich connective tissue (E). (F) Erectors are closely associated with collagen where they attach to the basement membrane of the epidermis. Tissue types were identified by stain affinities and morphology: ch, chromatophore; dem.c, circular dermal erector muscle; coll, collagen; dem, dermal erector muscle; dem.h, horizontal dermal erector muscle; ep, epidermis; muc, mucus; ref, reflective elements; ret, retractor muscle. Scale bars: 100 μm.

SEM

Sections of *O. bimaculoides* arm papillae and *S. apama* face ridge papillae were dewaxed with an ethanol series (100% for 5 min, 95%, 85%, 70%, 85%, 95% for 2 min each, three changes of 100% for 30 min each), treated with three changes of approximately 250 μl hexamethyldisilazane, and allowed to dry overnight in a hood (Bray et al., 1993). Slides were sputter coated with 7.5 nm of platinum and imaged with a Zeiss Supra 40VP SEM.

RESULTS

Sepia officinalis—Small Dorsal Papillae

In *Sepia officinalis*, small dorsal papillae are small, conical, and found on the dorsal surface of the mantle, face, and arms (Fig. 1A,B). Putative retractor muscles (hereafter, "retractors") were found extending from the papilla's apex to its base
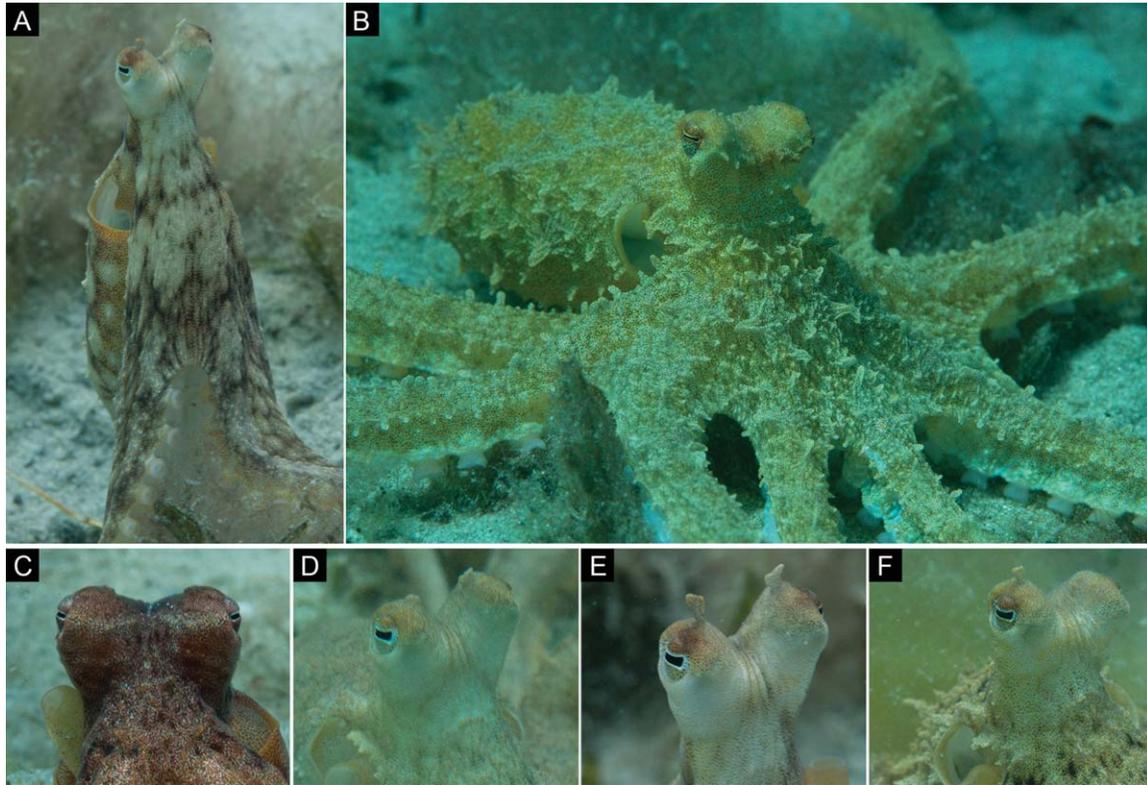
Fig. 4. *Macrotritopus defilippi* showing smooth (**A**) and papillate (**B**) skin. (**C–E**) The pair of dorsal eye papillae can range from retracted to extended and can be expressed unilaterally (**F**).

(Fig. 1C–I). In one series, a retractor bundle branched near the papilla's apex (Fig. 1I). Staining with Müller's colloidal iron and Van Gieson's stain revealed a layer of mucopolysaccharide-rich connective tissue (carboxymucins) between the muscle fibers making up the muscular core (Fig. 1I,J). In the extrapapillary skin, this layer persisted between the collagen layer and the layer of leucophores and iridophores (hereafter, "reflective elements"). Blood vessels (Fig. 1J) and nerves (Fig. 1C–E) were found near the base of the papilla.

Octopus vulgaris—Small Dorsal Papillae, Ventral Eye Papillae

Octopus vulgaris small dorsal papillae are small, conical, and found on the surface of the mantle, face, and arms; three ventral eye papillae are found below each eye (Fig. 2A–D). *En face* serial sections of partially extended small dorsal papillae revealed two sets of erector muscles: horizontal dermal erector muscles (hereafter, "horizontal erectors") and concentric circular dermal erector muscles (hereafter, "circular erectors"). Horizontal erectors spanned the width of the papilla (Fig.

2F,G) while circular erectors traced the papilla's circumference (Fig. 3A–C). The horizontal erectors traveled in bundles between overlying reflectors and chromatophores to attach to the basement membrane of the epidermis. This arrangement occurred in both small dorsal and ventral eye papillae (Figs. 2E–H,J and 3E,F). In small dorsal papillae, retractors radiated outward from the center of the muscular core and attached to the circular erectors (Figs. 2I and 3A–C). Both circular and horizontal erectors exhibited obliquely striated myofilament arrangements (Fig. 2I,J). In retracted ventral eye papillae, the apparent space between muscle and collagen fibers (Fig. 3D) was filled with abundant mucopolysaccharide-rich connective tissue (Fig. 3E,F). Blood vessels and nerves were found near the base of the papillae (Fig. 2G).

Macrotritopus defilippi—Dorsal Eye Papillae

Macrotritopus defilippi dorsal eye papillae are a pair of supraocular papillae (Fig. 4A–F). The core of these papillae was composed of horizontal erectors supported by mucopolysaccharide-rich connective tissue (Fig. 5A–F). Sparse bundles of erectors passed through the reflective element and
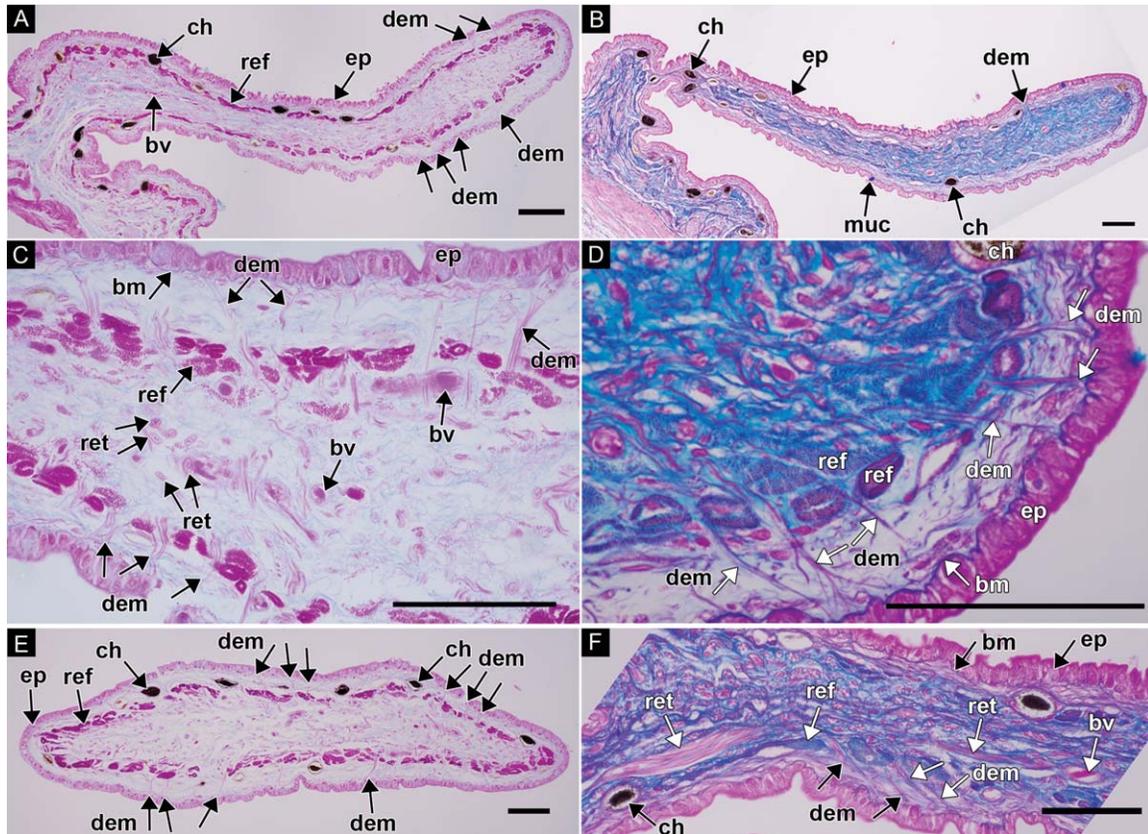
Fig. 5. (**A–F**) *Macrotritopus defilippi* dorsal eye papillae. (A,C,E) Mallory's triple connective tissue stain. (B,D,F) Müller's colloidal iron and Van Gieson's stains. (A,B) Dorsal eye papilla cut in cross section showing papilla elements (A) and the presence of mucopolysaccharide-rich connective tissue (B). (C,D) Higher magnification views of *en face* (C) and cross sections (F) showing fine, sparse erectors passing between the reflective elements and chromatophore layers to attach to the basement membrane of the epidermis. (E) *En face* section showing papilla elements. (F) In cross sections, retractors were found parallel with the long axis of the papilla; in *en face* sections, retractors were found cut in cross section (C). Tissue types were identified by stain affinities and morphology: bm, basement membrane; bv, blood vessel; ch, chromatophore; dem, dermal erector muscle; ep, epidermis; muc, mucus; ref, reflective elements; ret, retractor muscle. Scale bars: 100 μm.

chromatophore layers to attach to the basement membrane of the epidermis (Fig. 5C,D). Retractors were found parallel to the papilla's main axis (Fig. 5C,F). Blood vessels (Fig. 5A,C) and nerves were found near the base of the papilla.

Abdopus aculeatus—Major Mantle Papillae

Abdopus aculeatus major mantle papillae are large, irregularly shaped and found on the dorsal and lateral surfaces of the mantle (Fig. 6A). The apical tip was capped with reflective elements (Fig. 6B,D) and composed of horizontal erectors (Figs. 6C–E and 7) supported by mucopolysaccharide-rich connective tissue (Figs. 6E and 7B). Bundles of erectors passed through the reflective elements and chromatophore layers to attach to the basement membrane of the epidermis (Fig. 8A,B,E). In the main axis, muscles were wrapped with collagen and mucopolysaccharide-rich connective tissue (Figs. 7B and 8C). Toward

the base of the papilla, circular erectors surrounded the main axis (Fig. 8D,F). Retractors were found parallel to the main axis (Fig. 7). Blood vessels and nerves were found near the base of the papilla (Fig. 8F).

Octopus bimaculoides—Arm, Minor Mantle, Dorsal Eye Papillae

Octopus bimaculoides arm papillae are small, conical, and are found on the dorsal side of each arm (Fig. 9B, green arrow), minor mantle papillae (Fig. 9B, blue arrow) are rounded and interspersed among major mantle papillae on the mantle, and dorsal eye papillae are compound, supraocular papillae (Fig. 9B, white arrow). Arm (Fig. 9D–F) and minor mantle (Fig. 9C,G,H) papillae contained a central mass of erectors surrounded by collagen (Fig. 9E,G,H) and mucopolysaccharide-rich connective tissue (Fig. 9D,F). In *en face* sections, circular erectors were identified, particularly in more basal
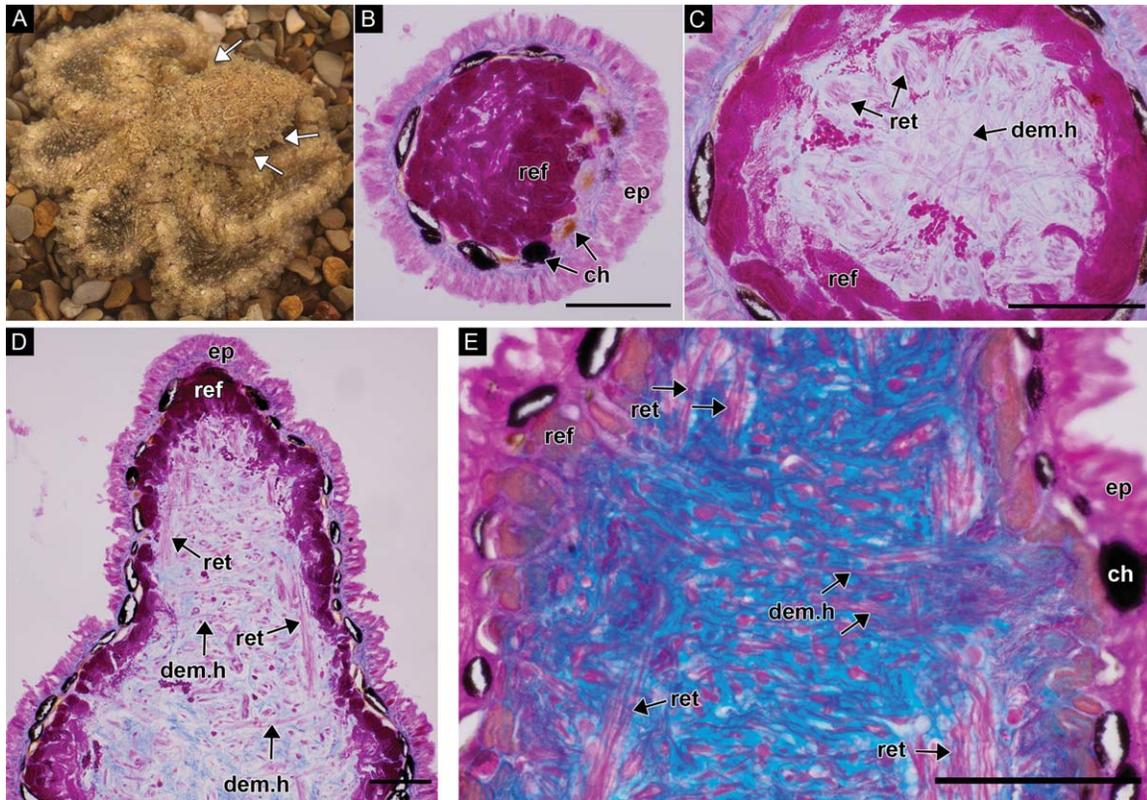
Fig. 6. (**A**) *Abdopus aculeatus* showing papillate skin; white arrows indicate lateral major mantle papillae. (**B–E**) Histology images. (B–D) Mallory's triple connective tissue stain, (E) Müller's colloidal iron and Van Gieson's stains. Papilla's apex *en face* (B,C) or in cross section (D,E). (B) Reflective elements at the apex. (C) Horizontal dermal erector muscles extend across the papilla's diameter near its apex; retractor muscles are cut in cross section in this orientation. (D,E) Cross sections of the papilla's apex, horizontal erectors extend from one side of the papilla to the other while retractors lie under the reflective elements layer, perpendicular to the horizontal erectors. Tissue types were identified by stain affinities and morphology: ch, chromatophore; ep, epidermis; dem.h, horizontal dermal erector muscle; ref, reflective elements; ret, retractor muscle. Scale bars: 100 μm.

sections and along the perimeter of the muscular core (Fig. 9C,D). However, horizontal erectors were more common. Erector bundles were sparse and passed between reflective elements and chromatophores to attach to the basement membrane of the epidermis *via* collagen (Fig. 10). Collagen was also found interspersed among muscle fibers in the center of the papillae. In extended papillae, the angle of these central collagen fibers changed abruptly near the base of the muscular core. Within the core, the collagen fibers were oriented perpendicular to the muscle fibers while below the core they were parallel with the muscle fibers (Fig. 9E–G). Retractors were found near the collagen fibers, also perpendicular to the horizontal erectors that made up the muscular core (Fig. 9E). Blood vessels and nerves were found near the base of the papillae (Fig. 9E,F).

Octopus bimaculoides dorsal eye papillae are compound papillae composed of a large main axis surrounded by smaller, protruding bulbous nodes (Figs. 11A,B and 12). The apex of the main axis and each bulbous node contained densely packed erectors (Figs. 11A–C and 13A). Bundles of erectors passed through the reflective elements and chromatophore layers and attached to the basement membrane of the epidermis *via* collagen. Erectors extended horizontally across the diameter of the papilla's apex (Figs. 11C and 13A) and in a concentric circular pattern in the papilla's main axis (Figs. 11D, 12, and 13D). In the main axis, muscle cells were sparsely bundled together where they passed through the reflective elements and chromatophore layers to connect to the basement membrane of the epidermis *via* a substantial amount of collagen (Fig. 11D). At the attachment points between individual nodes and the main axis, nodular muscles formed a tight meshwork with muscles in the main axis (Figs. 12C and 13E). Retractor muscles were found in both the bulbous nodes (Figs. 11A and 13B) and the papilla's main axis (Figs. 11A,B and 13C). Collagen was found throughout the main axis and was interspersed among muscle cells in the nodes (Figs. 11A,B,D, 12, and 13B,F). A layer of mucopolysaccharide-rich connective tissue
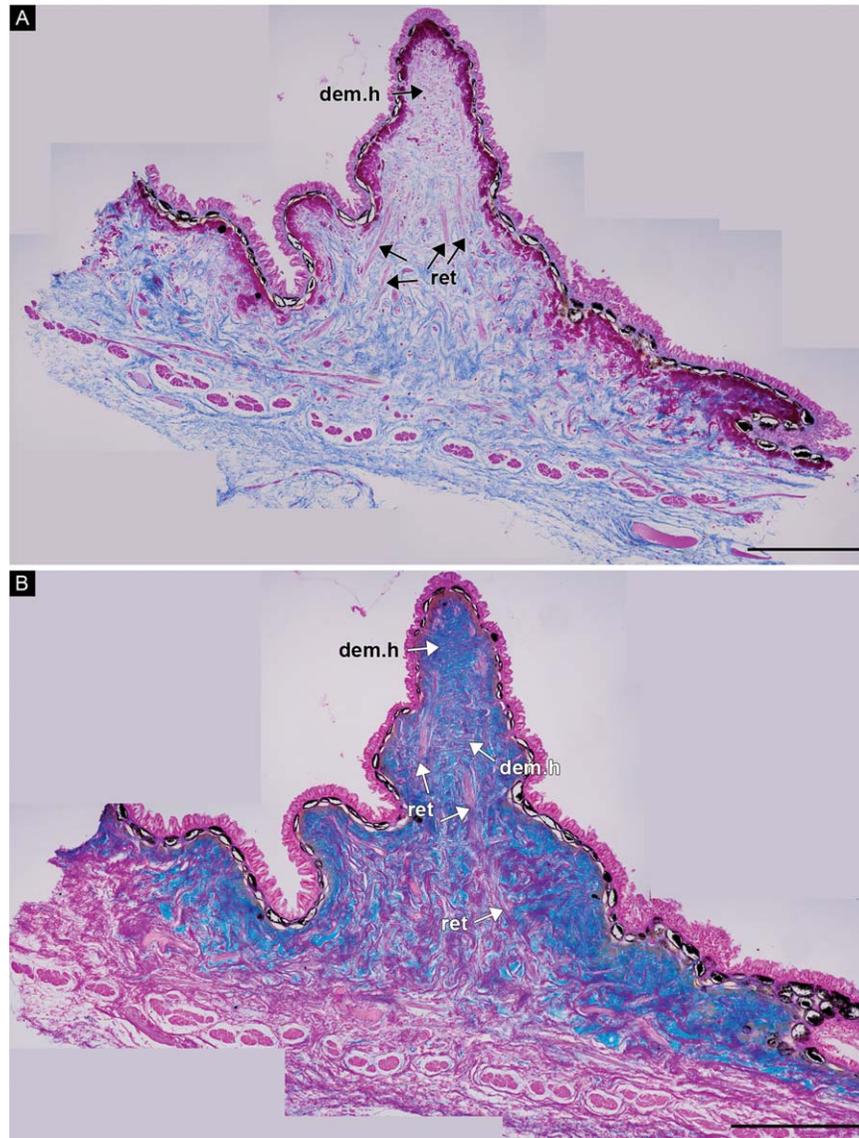
Fig. 7. *Abdopus aculeatus* major mantle papilla cut in cross section showing horizontal dermal erector muscles, retractor muscles and, in B, the distribution of mucopolysaccharide-rich connective tissue. (**A**) Mallory's triple connective tissue stain. (**B**) Müller's colloidal iron and Van Gieson's stains. Tissue types were identified by stain affinities and morphology: dem.h, horizontal dermal erector muscle; ret, retractor muscle. Scale bars: 500 μm.

surrounded the muscle cells in the apex and in each node (Figs. 11B, 12B,C, and 13D). Little mucopolysaccharide-rich connective tissue was found in the main axis of the papilla; that area was almost exclusively collagen (Figs. 11A,B, 12, and 13F). Blood vessels and nerves were found near the base of the papilla (Fig. 11A).

Sepia apama—Face Ridges

S. apama face ridge papillae cover the dorsal surface of the face and arms. Like other papillae, face ridges are typically extended in camouflage body patterns (Fig. 14A, animal on left, white arrow; Fig. 14B) and retracted during signaling

(Fig. 14A, animal on right) and swimming (Fig. 14C). The white lines that delineate the face ridges are the result of exposed reflective elements in the skin (Fig. 14A,B). Overlying chromatophores can be expanded to obscure these reflective elements (e.g., Fig. 14C). The chromatic components and the extension of the face ridge papillae are under independent neurological control. Long erectors extended across the width of each face ridge and passed between and below white leucophores before attaching to the basement membrane of the epidermis (Figs. 14D,E and 15A–D). Retractors extended from the margins of the reflective elements to the periphery (Fig. 15A). The bulk of an extended face ridge papilla was
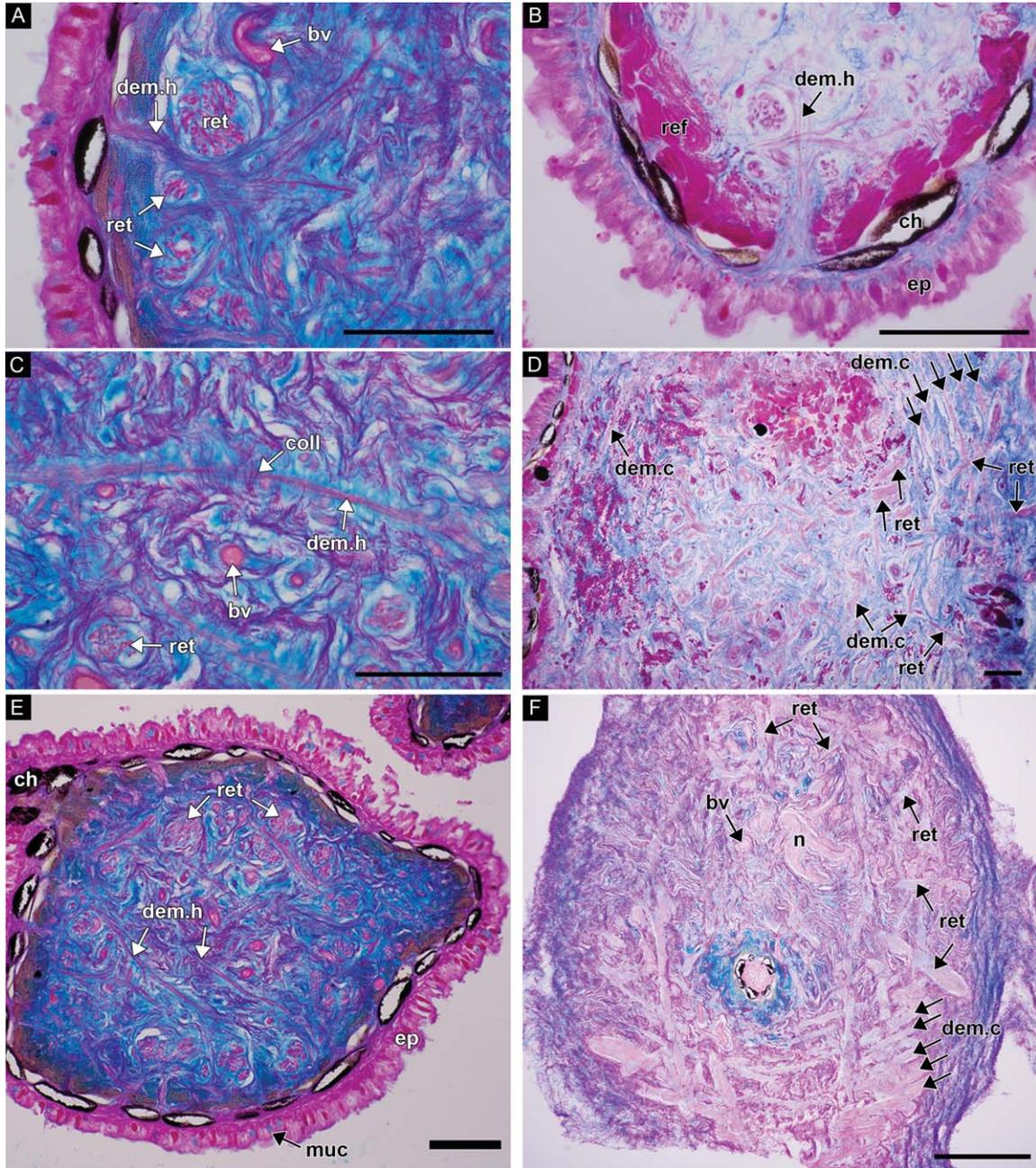
Fig. 8. (**A–F**) *En face* sections of *Abdopus aculeatus* major mantle papillae. (A,C,E) Müller's colloidal iron and Van Gieson's stains. (B,D,F) Mallory's triple connective tissue stain. (A,B) Bundles of erectors pass through the reflective elements and chromatophore layers to attach to the basement membrane of the epidermis. (C) Erector muscles are wrapped with collagen and mucopolysaccharide-rich connective tissue. (D,F) Circular erectors surround the periphery of the papilla near its base. (E) Horizontal erectors extend across the diameter of the papilla. In this orientation, retractors are cut in cross section. Tissue types were identified by stain affinities and morphology: bv, blood vessel; ch, chromatophore; coll, collagen; dem.c, circular dermal erector muscle; ep, epidermis; dem.h, horizontal dermal erector muscle; muc, mucus; n, nerve; ref, reflective elements; ret, retractor muscle. Scale bars: (A–E) 100 μm; (F) 500 μm.

composed of reflective elements (Figs. 14D,E and 15A). Leucophores were made up of whorls of spherical leucosomes, which were variable in size and staining pattern, and embedded in mucopolysaccharide-rich connective tissue (Fig. 15E–H). Blood vessels and nerves were found near the base of the papilla (Figs. 14D,E and 15A).

DISCUSSION
Functional Morphology

The functional morphology of each papilla type is summarized in a schematic diagram (Fig. 16). Cuttlefish (*S. officinalis*) small dorsal papillae and a possible mechanism of their extension have been
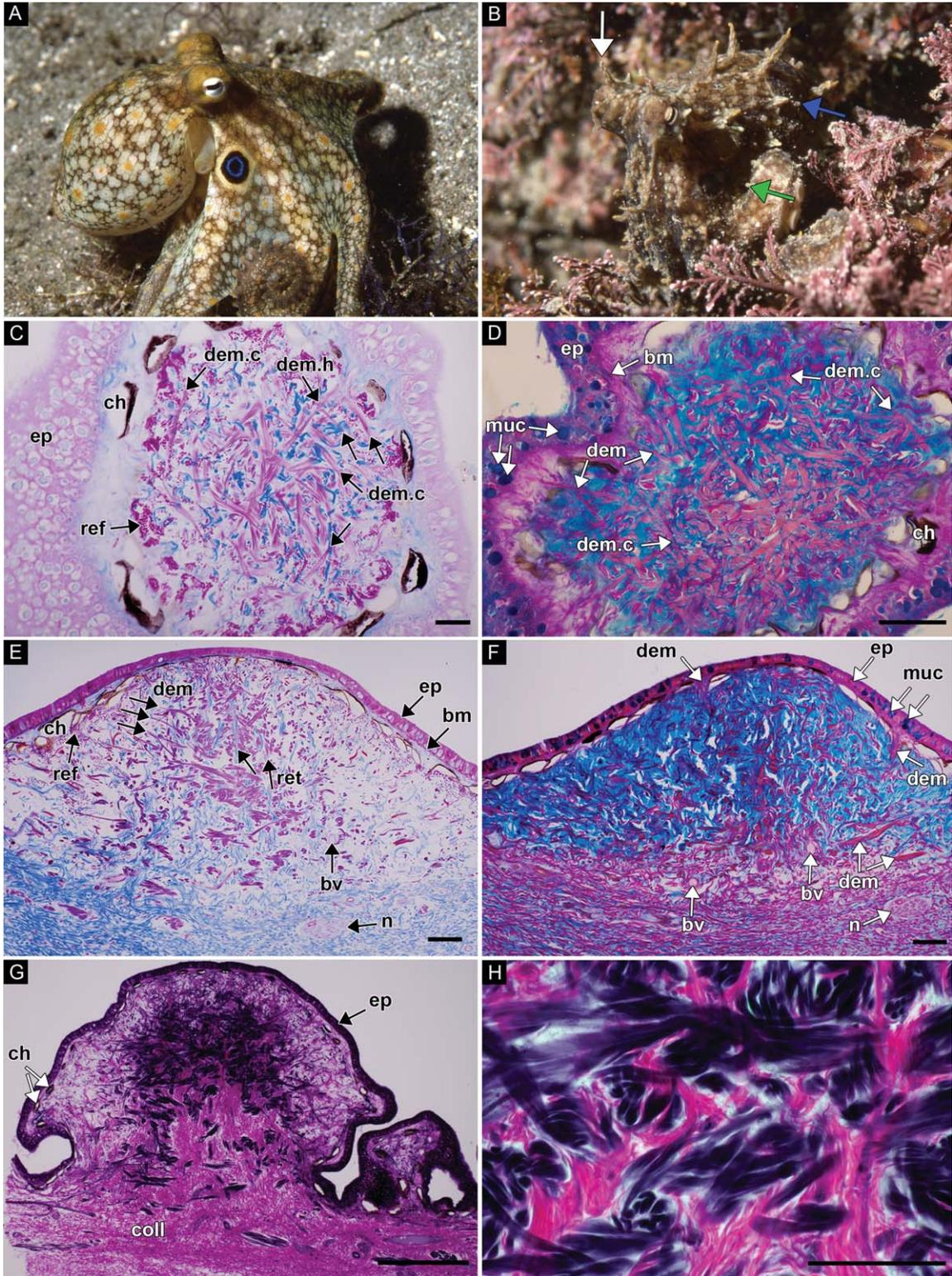
Fig. 9. *Octopus bimaculoides* showing smooth (**A**) and papillate (**B**) skin; arrows indicate arm (green), minor mantle (blue) and dorsal eye (white) papillae. (**C–H**) Histology images. (C,E) Mallory's triple connective tissue stain. (D,F) Müller's colloidal iron and Van Gieson's stains. (G,H) Verhoff's elastin and Van Gieson's stains. (C,G,H) Minor mantle papillae. (D–F) Arm papillae. (C,D) *En face* sections showing papilla elements, particularly circular and horizontal dermal erector muscles. (E–H) Cross sections showing papilla elements, particularly the dense muscular core, retractors (E) and vertically oriented collagen fibers (E–G). (D,F) The space surrounding the muscles in the muscular core is filled with mucopolysaccharide-rich connective tissue. (H) High magnification view of the muscular core in (G). Muscles (dark purple) are densely packed and interspersed with collagen (pink). Tissue types were identified by stain affinities and morphology: bm, basement membrane; bv, blood vessel; ch, chromatophore; coll, collagen; dem.c, circular dermal erector muscle; dem, dermal erector muscle; ep, epidermis; dem.h, horizontal dermal erector muscle; muc, mucus; ref, reflective elements; ret, retractor muscle. Scale bars: (C–F,H) 100 µm; (G) 500 µm.
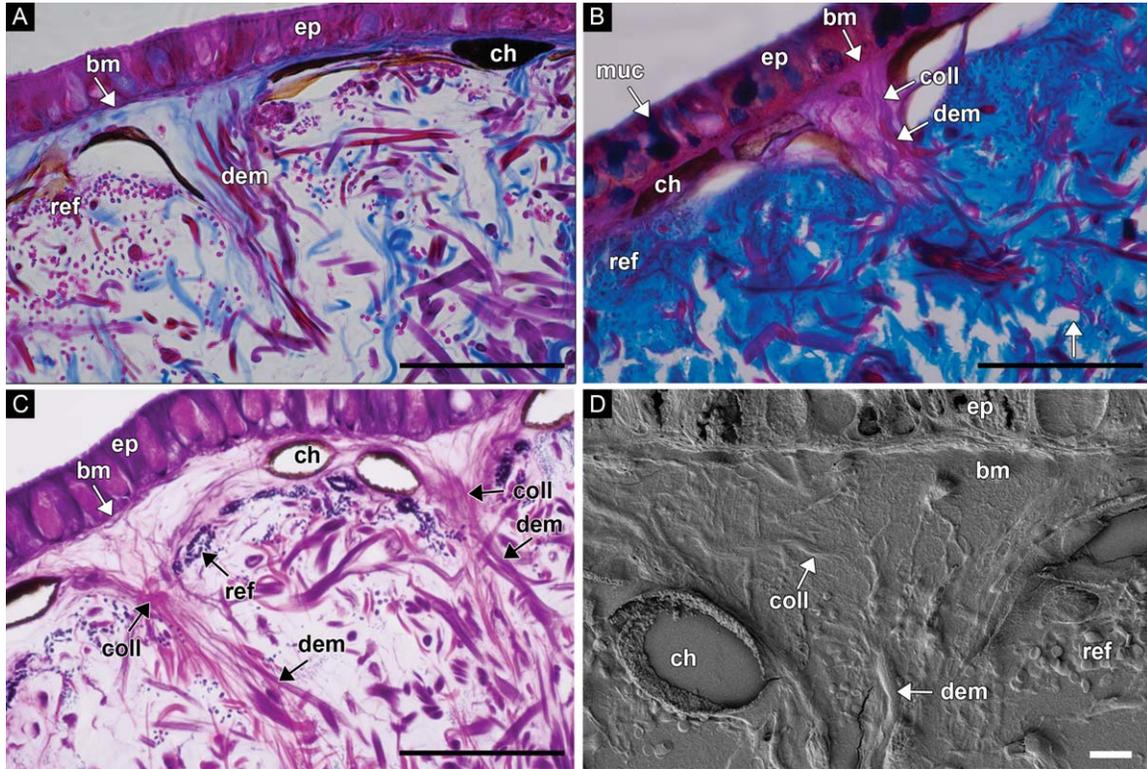
Fig. 10. *Octopus bimaculoides*. The connection point between the erectors and the basement membrane of the epidermis is mediated by collagen. (**A–D**) Cross sections. (A,B,D) Arm ridge papillae. (C) Minor mantle papilla. (A) Mallory's triple connective tissue stain. (B) Müller's colloidal iron and Van Gieson's stains. (C) Verhoff's elastin and Van Gieson's stains. (D) Scanning electron micrograph. Tissue types were identified by stain affinities and morphology: bm, basement membrane; ch, chromatophore; coll, collagen; dem, dermal erector muscle; ep, epidermis; muc, mucus; ref, reflective elements. Scale bars: (A-C) 100 μm; (D) 10 μm.

described (Allen et al., 2013). Briefly, circular erectors near the base of the papilla contract and shorten, reducing the circumference of their circular pattern. This shortening lifts the overlying tissues away from the body surface, extending the papilla. Simultaneous contraction of horizontal erectors pulls the perimeter of the papilla toward the center of its core as the horizontal erectors shorten from U-shaped in retracted papillae [see Allen et al. (2013) and, in octopus, compare Fig. 2E with 2F] to roughly parallel with the surface of the animal (horizontal). The contraction of the horizontal erectors likely contributes to extension as well as establishes the papilla's shape. The new results presented in this report show that additional components should be added to Allen et al.'s muscular hydrostat model of *S. officinalis* small dorsal papilla functional morphology: i) presence of mucopolysaccharide-rich connective tissue and ii) retractor muscles. The mucopolysaccharide-rich connective tissue surrounds the erectors and likely functions as a relatively incompressible hydrogel, helping to hold muscle cells together and assisting with structural support during extension. Although Allen et al. (2013) hypothesized that contraction of small, mesh-like subepidermal muscles

between the chromatophore layer and the epidermis might contribute to active papilla retraction, new results suggest that retractor muscles occur between the muscular core and the reflective elements layer in *S. officinalis* and all other papillae studied. This location, orientation and conservation suggest that these muscles are involved in active papilla retraction.

The organization of *Octopus vulgaris* papilla elements suggests they function like *S. officinalis* papillae. Contractions of basal circular erectors lift the papilla away from the mantle musculature while simultaneous contractions of horizontal dermal erector muscles pull the papilla's perimeter toward its core and determine its shape. In *en face* sections, retractor muscles attached to the circular dermal erector muscles and radiated from the center of the papilla to its perimeter like spokes on a wheel (Fig. 3A–C). In both *S. officinalis* and *O. vulgaris*, active papilla retraction might be accomplished similarly: retractors lie above and around the papilla's muscular core and their coordinated contraction likely pulls the apex of the papilla down toward its base while opposing and stretching the circular dermal erector muscles (Fig. 16A,B). Coordinated, active retraction versus
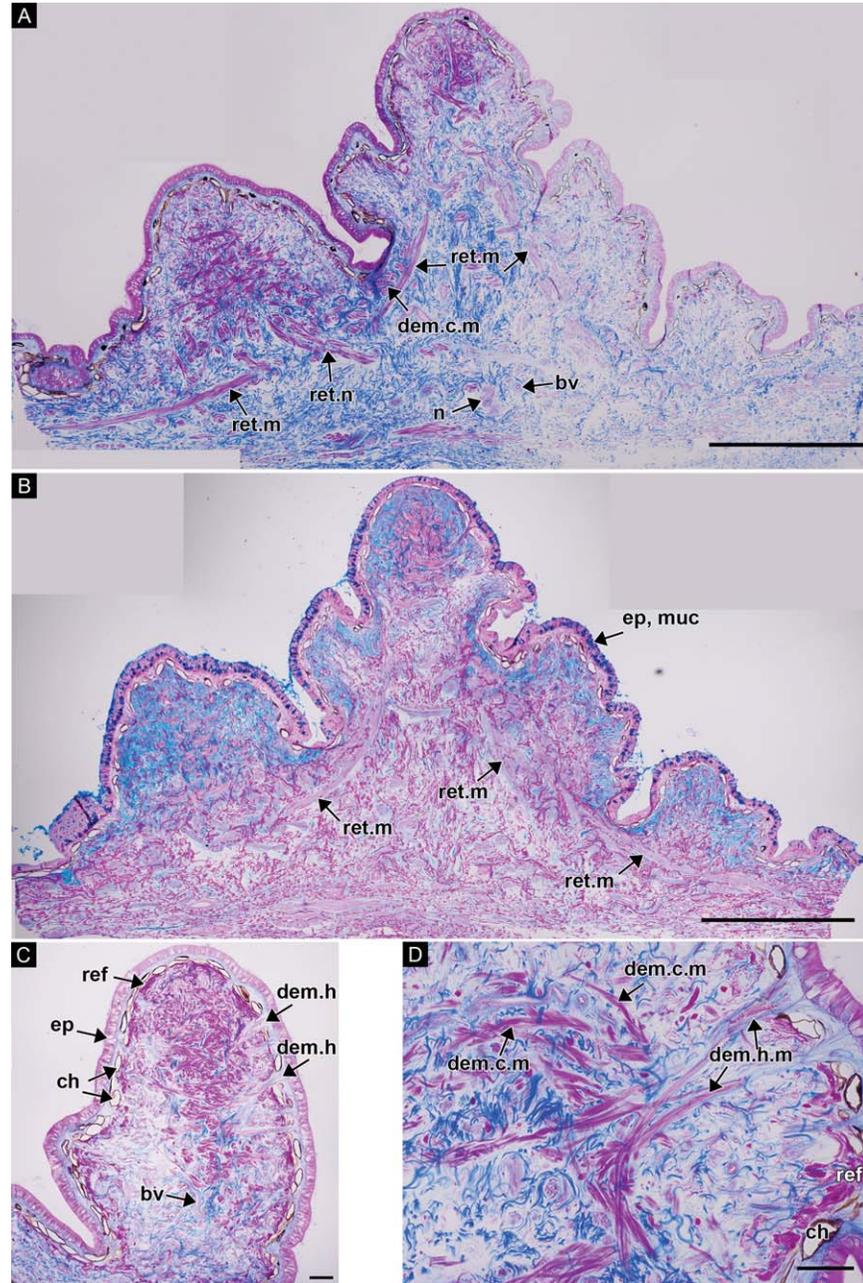
Fig. 11. (**A–D**) *Octopus bimaculoides* dorsal eye papillae in cross section (A–C) or *en face* (D). (A,C,D) Mallory's triple connective tissue stain. (B) Müller's colloidal iron and Van Gieson's stains. (A,B) The papilla's apex (C, higher magnification) and nodes were composed of densely packed erectors surrounded by collagen (blue in A,C; pink in B) and mucopolysaccharide-rich connective tissue (blue in B). The connective tissue in the papilla's main axis was predominantly collagen. Retractors were found for both the main axis (A,B) and individual nodes (A). (D) Circular erectors were found in the papilla's main axis. Horizontal erectors were attached to the basement membrane of the epidermis. Tissue types were identified by stain affinities and morphology: bv, blood vessel; ch, chromatophore; dem.c.m, circular dermal erector muscle that extends the main axis; dem.h, horizontal dermal erector muscle; dem.h.m, horizontal dermal erector muscle that shapes the main axis; ep, epidermis; n, nerve; ref, reflective elements; ret.m, retractor muscle for the main axis; ret.n, retractor muscle for a node. Scale bars: (A,B) 500 μm; (C,D) 100 μm.

elastic, rebound retraction is important for quickly smoothing the skin for reduced drag during swimming (Huffard, 2006), particularly for escape.

Macrotritopus defilippi dorsal eye papillae also appear to be muscular hydrostats; structural support is provided by muscle fibers surrounded by collagen and mucopolysaccharide-rich connective tissue (Fig. 5). The erectors were attached to the epidermal basement membrane but appeared sparse and loosely bundled where they passed through the reflective elements and chromatophore layers. This morphology was more similar to

O. bimaculoides arm and minor mantle papillae than to *S. officinalis* or *O. vulgaris* small dorsal papillae. Instead of circular erectors, *M. defilippi*

dorsal eye papillae were composed of many small, horizontally oriented erectors (Fig. 5C,D). Contraction of these muscles not only determines the papilla's flat, truncated shape, but by reducing its cross sectional diameter, it lengthens the papilla away from the dorsal surface of the eye [like the transverse muscles in squid tentacles, (Kier, 1982; Kier and Schachat, 2008)]. The opposing retractors were parallel with the long axis of the papilla (perpendicular to the horizontal dermal erector muscles); their contraction would shorten the long axis, retracting the papilla (Fig. 16C,D).

Externally, *Abdopus aculeatus* major mantle papillae appeared more complicated than the smaller, conical or rounded papillae examined here. Internally, however, these complex, three-dimensional skin structures contained the same three sets of muscles found in the simple papillae of *S. officinalis*, *O. vulgaris*, and *O. bimaculoides*: horizontal erectors, circular erectors, and retractors. Likewise, *A. aculeatus* major mantle papillae contained a matrix of mucopolysaccharide-rich connective tissue surrounding the erectors and collagen in the apex and main axis of the papilla and between the collagen and reflective elements layers in the periphery (Fig. 7). Unlike simple papillae, much of the main axis of *A. aculeatus* major mantle papillae was made up of collagen, similar to the compound dorsal eye papillae in *O. bimaculoides* (below). Although the muscles responsible for papilla extension and retraction likely function similarly to their corollaries in simple papillae (Fig. 16A,B), these more complicated papillae appear to rely more on structural support from collagen and mucopolysaccharide-rich connective tissue in the papilla's main axis rather than the structural support provided by cores of densely packed muscle cells in simple papillae.

O. bimaculoides arm and minor mantle papillae, although slightly larger than the *S. officinalis* and *O. vulgaris* small dorsal papillae, were comparatively similar in shape, complexity, and distribution of mucopolysaccharide-rich connective tissue. However, collagen in these simple papillae appeared to play a larger role than in the other species. Collagen was stretched through the region
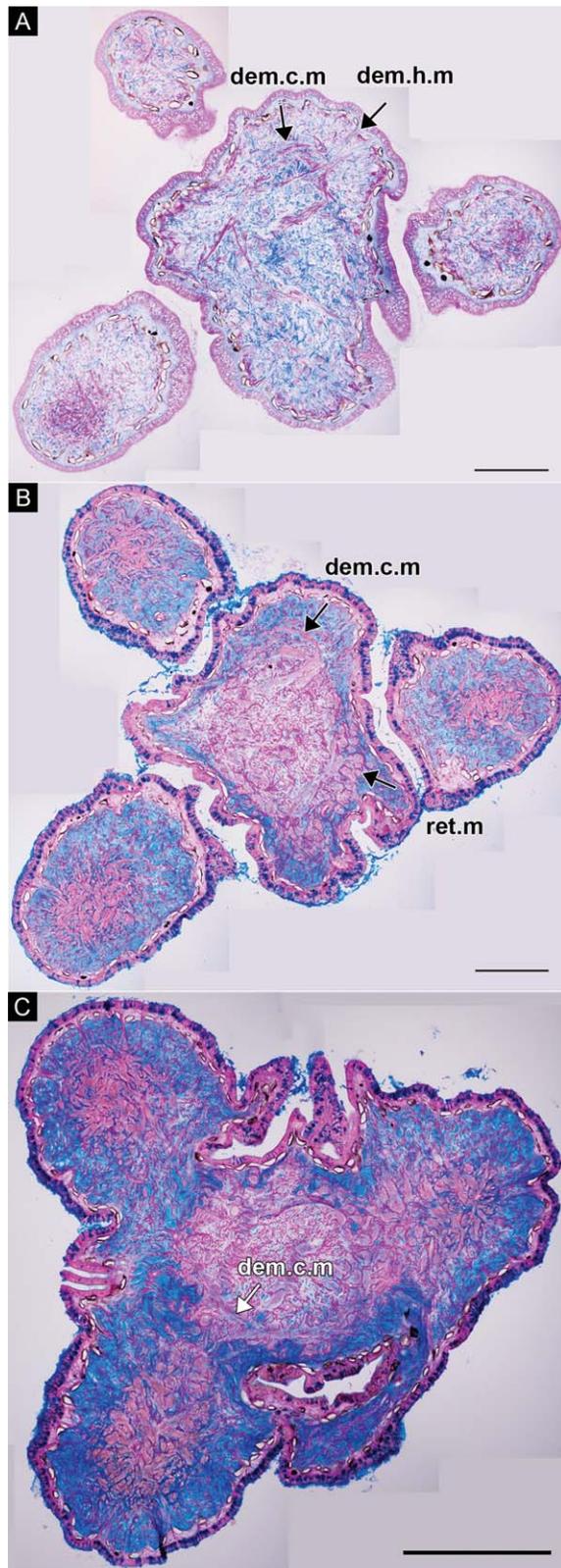
Fig. 12. *Octopus bimaculoides* dorsal eye papillae sectioned *en face* showing main axis surrounded by 3 nodes. (**A**) Mallory's triple connective tissue stain. (**B,C**) Müller's colloidal iron and Van Gieson's stains. The connective tissue in the papilla's main axis was predominantly collagen (blue in A, pink in B,C). Circular and horizontal erectors were found in the papilla's main axis. Retractors for the main axis were cut in cross section. Each node contained a dense, muscular core and, like the perimeter of the main axis, was surrounded by mucopolysaccharide-rich connective tissue (B,C). Tissue types were identified by stain affinities and morphology: dem.c.m, circular dermal erector muscle that extends the main axis; dem.h.m, horizontal dermal erector muscle that shapes the main axis; ret.m, retractor muscle for the main axis. Scale bars: 500 μm.
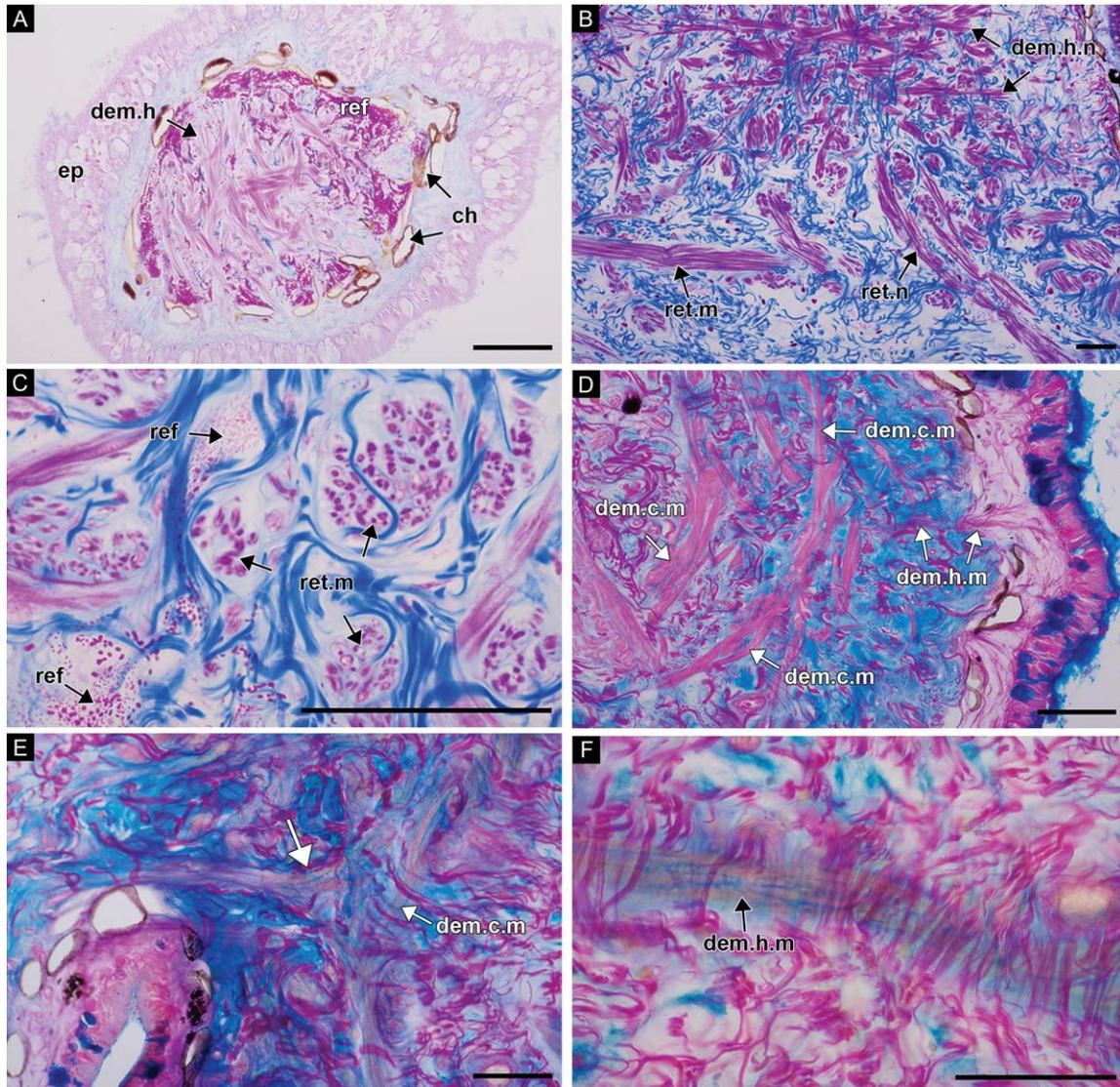
Fig. 13. *Octopus bimaculoides* dorsal eye papillae sectioned *en face* (**A,C–F**) or in cross section (**B**). (A–C) Mallory's triple connective tissue stain. (D–F) Müller's colloidal iron and Van Gieson's stains. (A) The papilla's apex contained horizontal erectors that extended across the diameter of the papilla. (B) One of the papilla's nodes. Each node was composed of densely packed erectors surrounded by collagen (blue). In cross section, this node appeared to have a retractor. (C) Retractors for the main axis shown in cross section. (D) Circular erectors were found in the papilla's main axis. (E) Nodes were attached to the circular erectors, white arrow. (F) In the main axis, erectors were surrounded by collagen. Tissue types were identified by stain affinities and morphology: ch, chromatophore; dem.c.m, circular dermal erector muscle that extends the main axis; dem.h, horizontal dermal erector muscle; dem.h.m, horizontal dermal erector muscle that shapes the main axis; dem.h.n, horizontal dermal erector muscle that shapes a node, ep, epidermis; ref, reflective elements; ret.n, retractor muscle for a node. Scale bars: 100 μm.

where the erector bundles attached to the epidermal basement membrane (Fig. 10). Collagen fibers were also found interwoven between the erectors in the muscular core to a greater degree than any other papillae examined (e.g., Fig. 9H). In extended papillae, there was a marked difference in the angle of these collagen fibers in the muscular core compared with those beneath the papilla's base: the collagen fibers in the muscular core were oriented perpendicularly to the horizontal dermal erector muscles (vertically) while the collagen fibers below the papilla were oriented horizontally. This organizational difference suggested that contraction of the erectors stretched the collagen and changed its orientation as the papilla extended. In malleable cephalopod tissue, elastic collagen is an important source of stored energy to oppose muscle contraction and restore shape (Kier and Thompson, 2003). It is likely that these stretched fibers contribute to passive papilla retraction while the nearby retractor muscles provide active papilla retraction (Fig. 9E,G and 16A,B).

Octopus bimaculoides dorsal eye papillae are so far the only compound papillae whose functional morphology has been investigated. Unlike the flat, truncated dorsal eye papillae in *M. defilippi*, *O. bimaculoides* dorsal eye papillae have a large, main axis with several smaller bulbous nodes extending from the sides (Figs. 11A,B and 12). The organization of the skin elements in the apex of the papilla and in each node was very similar to the arrangement of the small dorsal papillae in *S. officinalis* and *O. vulgaris*. Structural support for the papilla was provided by erectors, collagen, and mucopolysaccharide-rich connective tissue. Around

the perimeter of the papilla's main axis, we found circular erectors like those that were found near the base of *S. officinalis* and *O. vulgaris* small dorsal papillae. These circular erectors contract around central collagen fibers, lengthening the papilla by decreasing its diameter. Simultaneously, muscles that make up each node contract to give the dorsal eye papilla its compound shape; each node acts like a small, simple papilla (Figs. 13B and 16E). Animals with compound papillae may have fine control of the main axis and nodes; *S. apama* have been observed extending their multilobate dorsal eye papillae in graded increments (Supporting Information Fig. S1). The shape of the nodes might also be influenced by contractions of the circular erectors in the main axis because they are directly linked *via* muscle and connective tissue fibers (Fig. 13E). Papilla retraction appears to be accomplished by passive and active components. Collagen, stretched during extension, stores energy that is released when the erectors relax. Simultaneously, each node is pulled back toward the main axis by the contraction of its own set of retractors (Figs. 13A and 16F) while the main axis of the papilla is actively pulled down toward the dorsal surface of the eye by large retractors on its perimeter (Figs. 11A,B and 16F).

Sepia apama face ridge papillae appear to extend *via* buckling rather than a muscular hydrostatic mechanism (Fig. 16G). A mass of leucophores embedded in mucopolysaccharide-rich connective tissue and capped with iridophores is lifted away from the subdermal musculature of the face and arms when the underlying erectors contract. These underlying muscles are attached to the basement membrane of the epidermis and lie perpendicular to the face ridge; their shortening causes the overlying skin layers to buckle upward. Because the reflectors and surrounding mucopolysaccharide-rich connective tissue are incompressible, their mass—not muscle tissue—supports the face ridge's three-dimensional shape. Active retraction appears
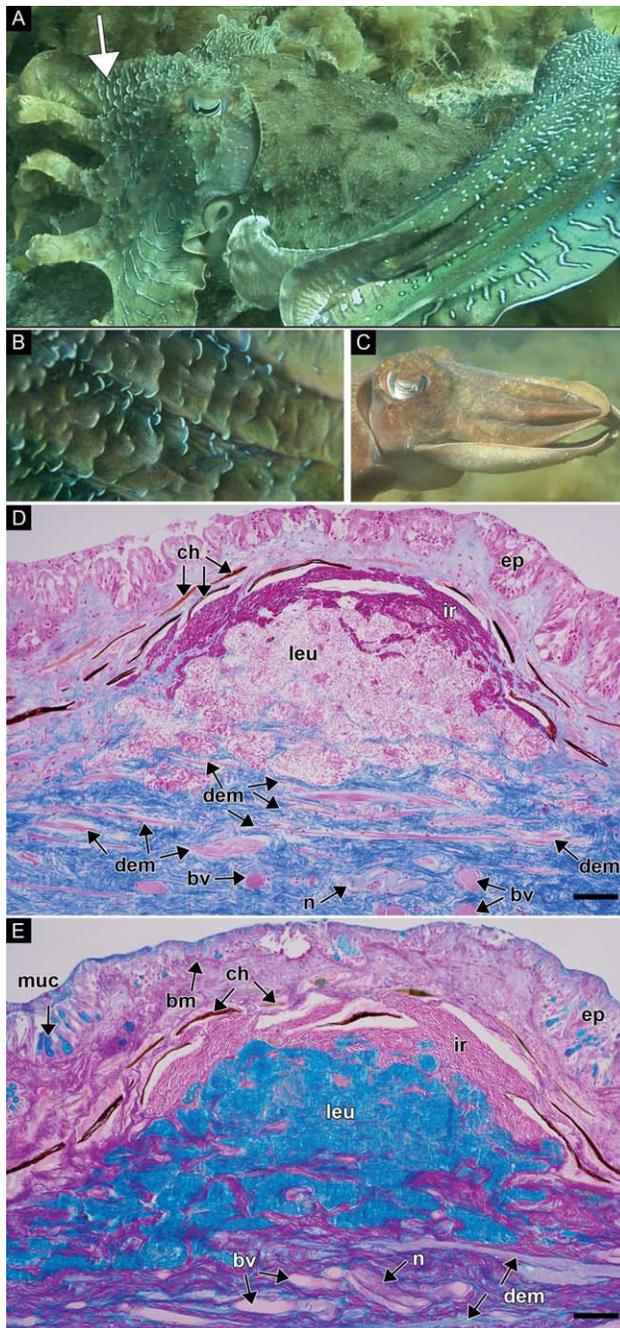
Fig. 14. *Sepia apama* face ridge papillae. (**A–C**) Field images of live animals. (A) In this species, the skin on the face and arms can appear rugose (animal on left, white arrow) or smooth (animal on right) due to the extension or retraction, respectively, of face ridge papillae. The animal on the right is engaged in signaling behavior. This skin texture is independent of the expression of reflective elements in the skin (white lines on the face of both animals). (B) Tight angle view of extended face ridge papillae. (C) A swimming animal showing smooth arms; reflective elements are obscured by overlying chromatophores. (**D,E**) Face ridge papilla in cross section. (D) Mallory's triple connective tissue stain. Dermal erector muscles underlie a mass of leucophores and iridophores, perpendicular to the ridge. (E) Müller's colloidal iron and Van Gieson's stain. Leucosomes are held in place by mucopolysaccharide-rich connective tissue. Tissue types were identified by stain affinities and morphology: bm, basement membrane; bv, blood vessel; ch, chromatophore; dem, dermal erector muscle; ep, epidermis; ir, iridophore; muc, mucus; leu, leucophore; n, nerve. Scale bars: 100 μm.
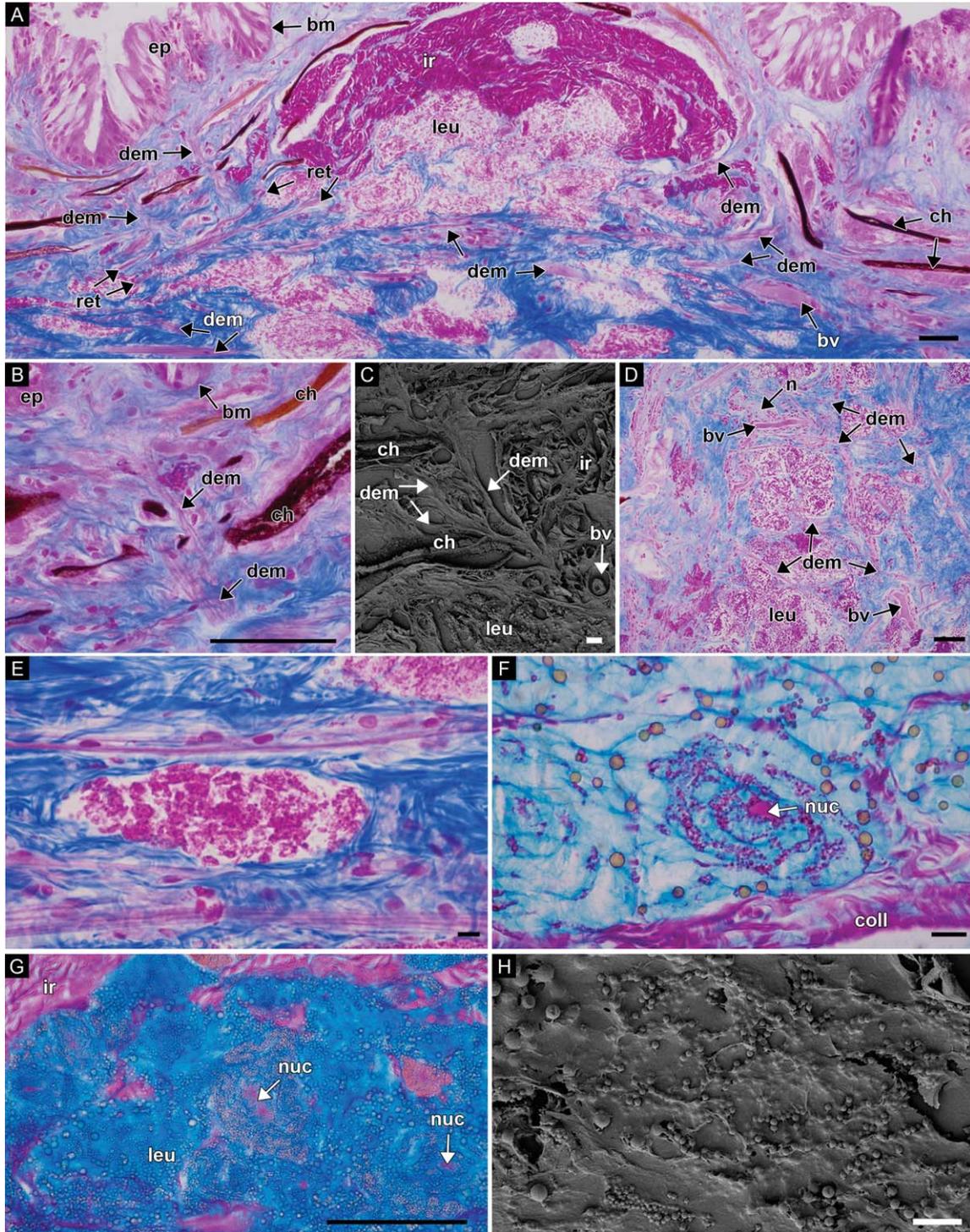
Fig. 15. (**A–H**) *Sepia apama* face ridge papillae. (A,B,D,E) Mallory's triple connective tissue stain. (C,H) Scanning eletron micrograph. (F,G) Müller's colloidal iron and Van Gieson's stain. (A) Dermal erector muscles attach to the basement membrane of the epidermis. Perpendicular to the erectors, retractors inserted near the perimeter of the reflective elements. (B,C) Erectors pass between chromatophores to radiate and (B) connect to the basement membrane of the epidermis. (D) *En face* section. Erectors underlie the reflective elements mass, perpendicular to the ridge. (E–H) Leucophores contain whorls of leucosomes. (F,G) Staining with Müller's colloidal iron and Van Gieson's stain revealed that dispersed leucosomes are contained within a mucopolysaccharide-rich connective tissue. In some leucophores, the nucleus could be discerned. (H) Scanning electron micrograph of leucophore containing leucosomes in a variety of sizes. Tissue types were identified by stain affinities and morphology: bm, basement membrane; bv, blood vessel; ch, chromatophore; dem, dermal erector muscle; ep, epidermis; ir, iridophore; leu, leucophore; nuc, nucleus; ret, retractor muscle. Scale bars: (A,B,D,G) 100 μm; (C,E,F,H) 10 μm.

Extended   **Retracted**
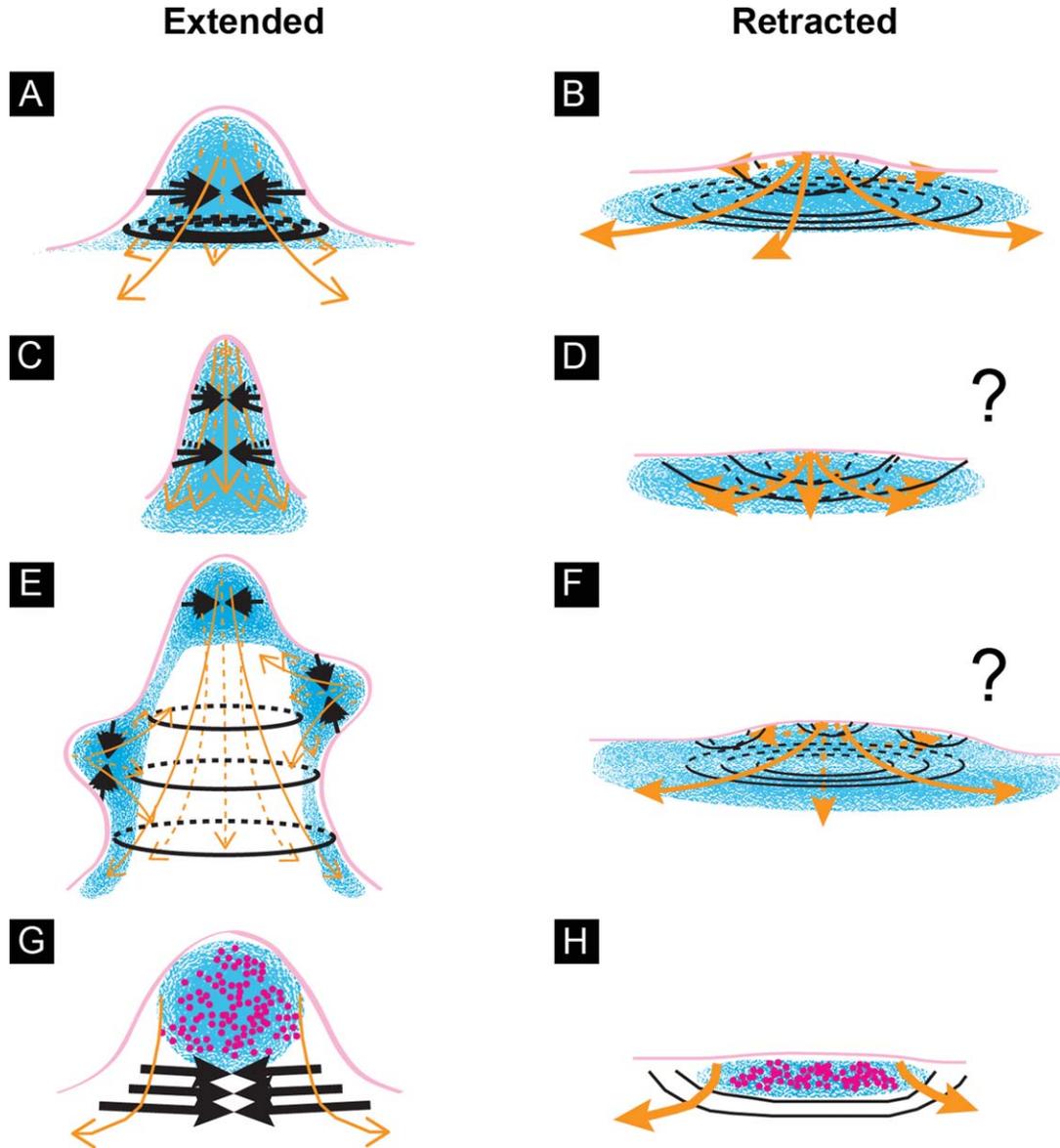
Fig. 16. Schematic drawings illustrating the functional morphology of four papilla types. Black lines represent erector muscles, orange lines, retractor muscles. Line thickness indicates contracted (thick) or relaxed (thin) muscle groups. Blue, mucopolysaccharide-rich connective tissue; collagen is not shown. The epidermis is represented by a pink line. Left column, extended papillae. Right column, retracted papillae. (**A,B**) Simple papilla: *Sepia officinalis* small dorsal papilla, *Octopus vulgaris* small dorsal and ventral eye papillae, *Abdopus aculeatus* major mantle papillae, *O. bimaculoides* arm and minor mantle papillae. (**C,D**) *Macrotritopus defilippi* spatulte, truncated dorsal eye papilla. (**E,F**) *O. bimaculoides* compound dorsal eye papilla. N.B., for graphic simplicity, node retractors are not shown in (F). (**G,H**) *S. apama* face ridge papilla, cross section.

to be accomplished by opposing retractor muscles on the edges of the reflective elements; contraction of these muscles likely widens and flattens the reflective elements mass, stretching the overlying connective tissue between the chromatophore layer and the epidermis (Fig. 16H).

Reflective Elements and Mucopolysaccharide-Rich Connective Tissue

Skin coloration and patterning are essential for camouflage and signaling. In all papillae, we found reflective elements (iridophores and leucophores) in a layer between the papilla's inner muscular core and the outer chromatophore layer (excluding *S. apama* face ridge papillae where the bulk of the papilla was made up of leucophores). Reflective elements were diverse in shape, size, and density but were consistent in staining pattern among animals (except among some *S. apama* leucosomes); their morphology, location, and spectral properties probably vary according to the ecology of the species, a topic that deserves future study.

Previous work suggested that the space between dermal erector muscles that make up the muscular hydrostatic core in *S. officinalis* small dorsal papillae might be filled with hemolymph (Allen et al., 2013). However, in all papillae examined, staining with Müller's colloidal iron and Van Gieson's stain showed that much of the space between muscle fibers is instead occupied by mucopolysaccharide-rich connective tissue. The biochemical makeup, density, and structure of this tissue could not be determined with our staining methods but it appears that this mucopolysaccharide-rich connective tissue provides an extracellular matrix for dispersed leucosomes in *S. apama* and, along with erector muscles, is an incompressible, supportive element for all other papillae studied. The layer of mucopolysaccharide-rich connective tissue persisted between the underlying collagen and overlying reflective elements layer outside the perimeter of the papillae studied and possibly functions as a hydrogel. In any case, it is likely that this mucopolysaccharide-rich connective tissue skin layer has important mechanical properties in the malleable skin of these animals.

In summary, this article focused on the comparative functional morphology of several papilla types in two cuttlefish and four octopus species. With the exception of *S. apama* face ridge papillae, which likely function *via* skin buckling, it appears that cuttlefish and octopus papillae are muscular hydrostats. Each papilla is composed of musculature and connective tissue that provide structural support while allowing fine, dynamic control of the skin's three-dimensional texture.

ACKNOWLEDGEMENTS

LITERATURE CITED

Akkaynak D, Allen JJ, Mäthger LM, Chiao C-C, Hanlon RT. 2012. Quantification of cuttlefish (*Sepia officinalis*) camouflage: A study of color and luminance using in situ spectrometry. J Comp Physiol A 199:211–225.

Allcock AL. 2005. On the confusion surrounding *Pareledone charcoti* (Joubin, 1905) (Cephalopoda: Octopodidae): Endemic radiation in the Southern Ocean. Zool J Linn Soc 143:75–108.

Allen JJ, Mäthger LM, Barbosa A, Hanlon RT. 2009. Cuttlefish use visual cues to control 3-dimensional skin papillae for camouflage. J Comp Physiol A 195:547–555.

Allen JJ, Bell GRR, Kuzirian AM, Hanlon RT. 2013. Cuttlefish skin papilla morphology suggests a muscular hydrostatic function for rapid changeability. J Morphol 274:645–656.

Barbosa A, Florio CF, Chiao CC, Hanlon RT. 2004. Visual background features that elicit mottled body patterns in cuttlefish, *Sepia officinalis*. Biol Bull 207:154.

Barbosa A, Mäthger LM, Buresch KC, Kelly J, Chubb C, Chiao C-C, Hanlon RT. 2008. Cuttlefish camouflage: The effects of substrate contrast and size in evoking uniform, mottle or disruptive body patterns. Vis Res 48:1242–1253.

Barbosa A, Allen JJ, Mäthger LM, Hanlon RT. 2012. Cuttlefish use visual cues to determine arm postures for camouflage. Proc R Soc B 279:84–90.

Boyle PR, Boletzky SV. 1996. Cephalopod populations: Definition and dynamics. Philos Trans R Soc B 351:985–1002.

Bray DF, Bagu J, Koegler P. 1993. Comparison of hexamethyldisilazane (HMDS), Peldri II, and critical-point drying methods for scanning electron microscopy of biological specimens. Microsc Res Tech 26:489–495.

Bush SL, Robison BH, Caldwell RL. 2009. Behaving in the dark: Locomotor, chromatic, postural, and bioluminescent behaviors of the deep-sea squid *Octopoteuthis deletron* Young 1972. Biol Bull 216:7–22.

Chiao C-C, Chubb C, Hanlon RT. 2007. Interactive effects of size, contrast, intensity and configuration of background objects in evoking disruptive camouflage in cuttlefish. Vis Res 47:2223–2235.

Chiao C-C, Chubb C, Buresch K, Siemann L. 2009. The scaling effects of substrate texture on camouflage patterning in cuttlefish. Vis Res 49:1647–1656.

Chiao C-C, Chubb C, Buresch KC, Barbosa A, Allen JJ, Mäthger LM, Hanlon RT. 2010. Mottle camouflage patterns in cuttlefish: Quantitative characterization and visual background stimuli that evoke them. J Exp Biol 213:187–199.

Clarke MR. 1996. Cephalopods as prey. III. Cetaceans. Philos Trans R Soc B 351:1053–1065.

Cott HB. 1940. Adaptive Coloration in Animals. London: Methuen.

Croxall JP, Prince PA. 1996. Cephalopods as prey. I. Seabirds. Philos Trans R Soc B 351:1023–1043.

Hanlon RT. 2007. Cephalopod dynamic camouflage. Curr Biol 17:R400–R405.

Hanlon RT, Messenger JB. 1996. Cephalopod Behaviour. Cambridge: Cambridge University Press. pp 232.

Hanlon RT, Messenger JB. 1988. Adaptive coloration in young cuttlefish (*Sepia officinalis* L.): The morphology and development of body patterns and their relation to behaviour. Philos Trans R Soc Lond B 320:437–487.

Hanlon RT, Chiao C-C, Mäthger LM, Barbosa A, Buresch KC, Chubb C. 2009. Cephalopod dynamic camouflage: Bridging the continuum between background matching and disruptive coloration. Philos Trans R Soc Lond B 364:429–437.

Hanlon RT, Watson AC, Barbosa A. 2010. A "mimic octopus" in the Atlantic: Flatfish mimicry and camouflage by *Macrotritopus defilippi*. Biol Bull 218:15–24.

Hanlon RT, Chiao C-C, Mäthger LM, Buresch KC, Barbosa A, Allen JJ, Siemann L, Chubb C. 2011. Rapid adaptive camouflage in cephalopods. In: Stevens M, Merilaita S, editors. Animal Camouflage: Mechanisms and Function. Cambridge: Cambridge University Press. pp 145–163.

Huffard CL. 2006. Locomotion by *Abdopus aculeatus* (Cephalopoda: Octopodidae): Walking the line between primary and secondary defenses. J Exp Biol 209:3697–3707.

Huffard CL, Boneka F, Full RJ. 2005. Underwater bipedal locomotion by octopuses in disguise. Science 307:1927.

Humason GL. 1967. Animal Tissue Techniques. San Francisco, London: W. H. Freeman and Company.

Kelman EJ, Baddeley RJ, Shohet AJ, Osorio D. 2007. Perception of visual texture and the expression of disruptive camouflage by the cuttlefish, *Sepia officinalis*. Proc R Soc B 274:1369–1375.

Kier WM. 1982. The functional morphology of the musculature of squid (*Loliginidae*) arms and tentacles. J Morphol 172:179–192.

Kier WM. 1992. Hydrostatic skeltons and muscular hydrostats. In: Biewener AA, editor. Biomechanics (Structures and

Systems): A Practical Approach. New York: IRL Press at Oxford University Press. p 205–231.

Kier WM. 2012. The diversity of hydrostatic skeletons. J Exp Biol 215:1247–1257.

Kier WM, Schachat FH. 2008. Muscle specialization in the squid motor system. J Exp Biol 211:164–169.

Kier WM, Smith KK. 1985. Tongues, tentacles and trunks: The biomechanics of movement in muscular-hydrostats. Zool J Linn Soc 83:307–324.

Kier WM, Stella MP. 2007. The arrangement and function of octopus arm musculature and connective tissue. J Morphol 268:831–843.

Kier WM, Thompson JT. 2003. Muscle arrangement, function and specialization in recent coleoids. Berl Paläobiol Abh 3: 141–162.

Klages NTW. 1996. Cephalopods as prey. II. Seals. Philos Trans R Soc B 351:1045–1053.

Mäthger LM, Chiao C-C, Barbosa A, Hanlon RT. 2008. Color matching on natural substrates in cuttlefish, *Sepia officinalis*. J Comp Physiol A 194:577–585.

Moynihan M, Rodaniche AF. 1982. The behavior and natural history of the Caribbean reef squid *Sepioteuthis sepioidea* with a consideration of social, signal, and defensive patterns for difficult and dangerous environments. Adv Ethol 25:1–150.

Norenburg JL, Barrett JM. 1987. Steedman's polyester wax embedment and de-embedment for combined light and scanning electron microscopy. J Electron Microsc Tech 6:35–41.

Norman MD, 2000. Cephalopods: A World Guide. Hackenheim: ConchBooks. pp 320.

Packard A, Hochberg FG. 1977. Skin patterning in *Octopus* and other genera. Symp Zool Soc Lond 38:191–231.

Packard A, Sanders GD. 1971. Body patterns of *Octopus vulgaris* and maturation of the response to disturbance. Anim Behav 19:780–790.

Roper CFE, Hochberg FG. 1988. Behavior and systematics of cephalopods from Lizard Island, Australia, based on color and body patterns. Malacologia 29:153–193.

Smale MJ. 1996. Cephalopods as prey. IV. Fishes. Philos Trans R Soc B 351:1067–1081.

Smith KK, Kier WM. 1989. Trunks, tongues, and tentacles: Moving with skeletons of muscle. Am Sci 77:28–35.

Stevens M, Merilaita S. 2009. Defining disruptive coloration and distinguishing its functions. Philos Trans R Soc Lond B 364:481–488.

Weaver HL. 1955. An improved gelatine adhesive for paraffin sections. Stain Technol 30:63–64.

Zylinski S, Johnsen S. 2011. Mesopelagic cephalopods switch between transparency and pigmentation to optimize camouflage in the deep. Curr Biol 21:1937–1941.

Zylinski S, Osorio D, Shohet AJ. 2009a. Cuttlefish camouflage: Context-dependent body pattern use during motion. Proc R Soc B 276:3963–3969.

Zylinski S, Osorio D, Shohet AJ. 2009b. Perception of edges and visual texture in the camouflage of the common cuttlefish, *Sepia officinalis*. Philos Trans R Soc B 364:439–448.